Avalanche processes in an idealized lamp: I. Measurements of formative breakdown time

Richard S Moss[1], J Gary Eden[2] and Mark J Kushner[2,3]

[1] Department of Mechanical and Industrial Engineering, University of Illinois,
1406 W Green St., Urbana, IL 61801, USA
[2] Department of Electrical and Computer Engineering, University of Illinois,
1406 W Green St., Urbana, IL 61801, USA

E-mail: mjk@uiuc.edu

Abstract
Electrical breakdown of cold (room temperature) metal-halide arc lamps
typically occurs through the fill of a rare gas (at a pressure of tens of Torrs)
and the vapour produced by the metal donor. Restarting a warm lamp is
often made difficult by the high pressure of the metal and metal-halide
vapours. To reliably start cold lamps with a minimum voltage and a
minimum sputtering of the electrodes, and to restart warm lamps that have a
high pressure of the metal and metal-halide vapours, auxiliary sources of
ionization are often used. As a point of departure for the study of these
processes, measurements of formative breakdown times were made in a
cylindrical discharge tube resembling a compact polycrystalline alumina
envelope metal-halide lamp. Breakdown times were measured for Ar/Xe
gas mixtures at total pressures of 10–90 Torr and biases up to 2 kV applied to
a 1.6 cm gap. The data provide a knowledge base for a companion
computational investigation. We found that breakdown times generally
decreased with small admixtures of Xe in Ar (5–15%) and increased with
larger admixtures. We attribute these trends to the changing shape of the tail
of the electron energy distribution.

1. Introduction

Metal-halide lamps typically operate in the steady state as
multi-atmosphere thermal arcs through a vapour provided by
doses of mercury and metal halides [1–8]. The cold fill of
the lamp is usually 10–100 Torr of a rare gas and the room
temperature vapour pressure of the dose. The anode-to-
cathode gaps are as small as a few millimetres in high pressure
lamps used for projectors, ≈1 cm for compact polycrystalline
alumina envelope lamps, and 3–5 cm in conventional quartz
envelope lamps. Optimizing the breakdown and avalanche
processes of both cold and warm lamps continues to be a
priority in the lamp community. Lowering the breakdown
voltage in cold lamps not only reduces the cost of the driving

electronics but also reduces electrode erosion by sputtering,
thereby extending the lamp lifetime. Another critical concern
is rapidly restarting a warm lamp, a process complicated by
the elevated pressure of the metal and metal-halide vapours,
which requires larger starting voltages.

Strategies for controlling and optimizing the breakdown
of metal-halide, high-intensity-discharge (HID) lamps were
recently reviewed in [9]. These strategies include preionization
using internal or external auxiliary electrodes or ultraviolet
(UV) radiation sources, spiker circuits to provide high-
voltage pulses with sub-microsecond rise times, and careful
placement of ground planes to optimize capacitive coupling
during breakdown. To improve our understanding of the
processes important to the breakdown phase of a discharge
under conditions representative of HID lamps (moderate gas
pressures but weak preionization), both experimental and

---

[3] Author to whom any correspondence should be addressed.

computational investigations were conducted in which Ar/Xe gas mixtures were used as a surrogate for the gas mixtures encountered when starting HID lamps. Ar/Xe mixtures have many of the same characteristics as, for example, the Ar/Hg mixtures found in actual lamps. In this paper, we report on measurements of breakdown and avalanche processes in a model lamp to provide a knowledge base for validation of a comprehensive plasma dynamics model. Results from the computational investigations are described in the companion paper, part II [10].

We found that the mean avalanche time is a sensitive function of the fraction of xenon in Ar/Xe mixtures over the range of pressures (10–100 Torr) and electric field strengths (400–1250 V cm^{-1}) investigated. Small admixtures of Xe (5–15%) in Ar reduced the mean avalanche time by factors as large as 3–4. The mean avalanche time recovered to the value in pure Ar with additions of $\approx$50% Xe. These trends are attributed to the smaller ionization potential of Xe, as compared with Ar, and Penning processes producing Xe$^+$ from highly excited states of Ar. Both of these processes increase the rate of ionization with small Xe fractions. With small admixtures of Xe, the tail of the electron energy distribution is not significantly perturbed, and so the lower threshold energy processes in xenon serve to increase the rate of ionization. The recovery of the mean avalanche time with large Xe fractions is attributed to the larger inelastic cross sections of Xe, as compared to Ar, which damp the tail of the electron energy distribution and so reduce the rate of ionization. The experimental apparatus will be described in section 2, followed by a discussion of mean avalanche times in Ar and Ar/Xe mixtures in sections 3 and 4. Our concluding remarks are in section 5.

2. Experimental apparatus

The experimental apparatus was designed to closely emulate commercially available polycrystalline alumina HID lamps [11]. A schematic of the lamp is shown in figure 1(a). It consisted of a 1 cm inner diameter quartz tube mounted between two grooved glass ceramic (Macor) substrates and sealed by Viton O-rings. Since breakdown characteristics are known to be sensitive to the proximity of ground planes, the lamp was geometrically isolated from these planes by a distance >30 cm. Tungsten electrodes $\approx$0.9 mm in diameter, identical to those in commercial HID lamps and supplied by APL Engineered Materials, were mounted through recessed holes in the ceramic flanges and set for a gap of 1.6 cm. The system was evacuated by a turbomolecular pump to a base pressure of 10^{-7} Torr (with a leak rate of less than a few milliTorrs per hour) and back filled with research grade Ar and Xe. All gas pressures cited here are room temperature values measured with a capacitance manometer. Access to the lamp for the vacuum and gas handling systems was provided by small ports in one of the ceramic flanges (not shown in figure 1(a)).

The electronics provided high-voltage pulses with controllable rise times at variable pulse repetition frequencies (PRFs). A pulse forming network, consisting of two insulated gate bipolar transistors driven by opto-isolators in conjunction with a digital delay generator, produced voltage pulses having nominal risetimes of 120 ns, widths up to 20 ms, and repetition
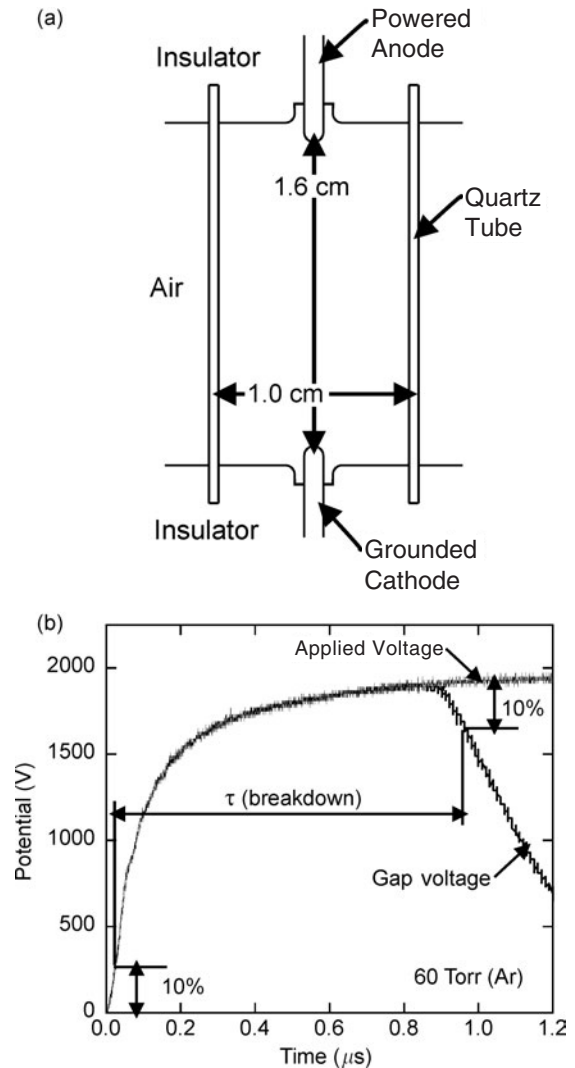
Figure 1. Experimental parameters. (*a*) Schematic of the apparatus. The top electrode was pulsed positive, while the lower electrode was grounded. (*b*) Typical applied voltage waveform and voltage waveform during breakdown. The breakdown time, τ, is the interval from 10% of the peak voltage prior to breakdown to the point at which the voltage has decreased by 10% from its peak value.

frequencies ranging from 0.1 Hz to 2 kHz. A typical applied voltage waveform is shown in figure 1(*b*). The positive voltage pulse was applied to the anode (upper electrode), with the cathode (lower electrode) at ground. A 11.5 kΩ series resistor provided ballasting. Breakdown was assessed based on voltage measurements made with a Tektronix P5100 probe. Voltage measurements were collected with and accumulated on a Tektronix TDS 5104 digital oscilloscope, with which signal analysis was also performed.

As discussed below, obtaining reproducible results having reasonable statistics required a source of preionization that, for these experiments, was provided by illuminating the discharge region with a mercury pen-lamp mounted a few centimetres from the quartz tube. The primary role of the UV ($\lambda \approx 254$ nm) illumination was to provide seed electrons at the electrodes and a background electron density of 10^5–10^6 cm^{-3}.

Each experiment was conducted by admitting a gas mixture of a predetermined composition and pressure to the

lamp chamber, setting the voltage and PRF of the power circuit, and pulsing the discharge until steady state conditions were achieved. Under these conditions, the breakdown time for the gas mixture was defined, as shown in figure 1(*b*), as the time interval between the 10% points (referenced to the maximum voltage sustained across the discharge) for both the rising and falling portions of the voltage waveform. The decrease in voltage across the gap, signifying the onset of breakdown, is due to the voltage drop across the ballast resistor when the plasma begins to draw significant current. A minimum of 300 breakdown measurements were made for each operating point and averaged in real time to provide the mean breakdown time, τ.

3. Base case conditions for breakdown in Ar

For a constant applied voltage, the breakdown time typically consists of two components, the statistical time lag and the formative time lag [12]. The statistical time lag is that time required to generate the initial seed electron(s) that start the avalanche. The formative time lag is the time required for the subsequent avalanche to increase the electron density of the plasma column to a value corresponding to a specified conductivity. The statistical time lag is a sensitive function of stochastic processes that produce the seed electrons and, hence, tends to have a large standard deviation. In contrast, the formative time lag is a function of the fundamental avalanche physics of the discharge and so has less scatter. In this work, the formative time lag is of greatest interest.

Operating the discharge at a high PRF and preionizing the gas mixture (as is the case in the experiments reported here) is ultimately a tradeoff between obtaining acceptable statistics in a reasonable collection time, and measuring the virgin avalanche characteristics; that is, one wishes to minimize the scatter in the statistical time lag while not prejudicing the measurement of the formative time lag. Operating at high repetition rates usually reduces the scatter in the statistical time lag by providing seed electrons from the previous pulse that have survived through the afterglow between pulses. High repetition rates also, unfortunately, produce gas heating and charging of surfaces that are, at best, difficult to characterize and, at worst, prejudice the outcome.

For example, mean breakdown times in argon are shown in figure 2(*a*) as a function of the repetition rate for 2000 V pulses for pressures of 30–70 Torr without UV illumination. Increasing the repetition rate decreases the scatter in the data, an effect attributable largely to eliminating scatter in the statistical time lag. Unfortunately, the increase in repetition rate also decreases τ. The reduction in τ is primarily the result of a reduction in the formative time lag due to an increase in the density of electrons that have survived from the previous pulse, and gas heating, which increases E/N (electric field strength/gas number density) for a given applied voltage. Argon atoms in the metastable 4s $[3/2]_2$ state (which have higher rates of ionization than the ground state) that survive from the previous pulse, and wall charging, which reduces the loss of electrons, are also likely to contribute to the decrease in τ. The decrease in mean breakdown time with increasing repetition rate has been previously quantified as a memory
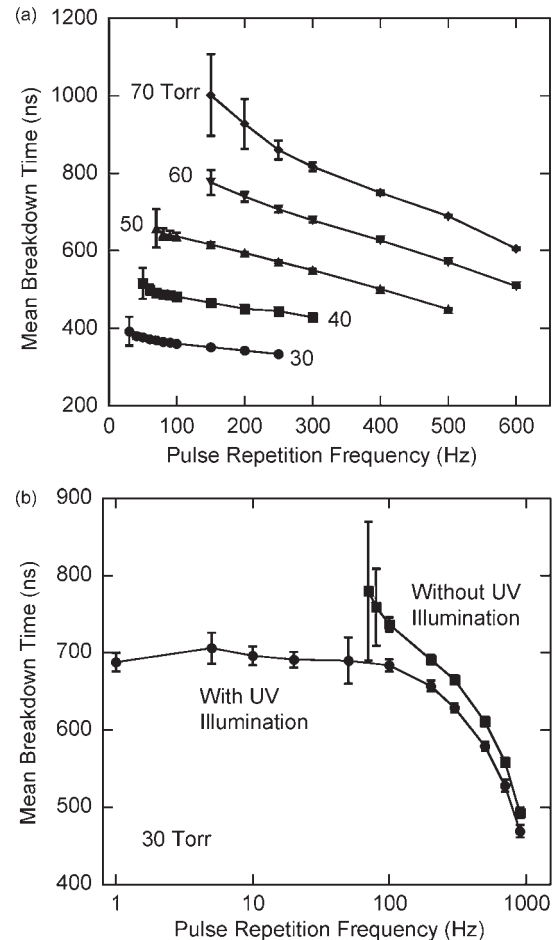
Figure 2. Mean breakdown times in pure argon as a function of pulse repetition rate. (*a*) τ for different pressures for 2000 V pulses. (*b*) τ with and without UV illumination at a pressure of 30 Torr for 1500 V pulses. The scatter in τ increases with decreasing repetition rate as the preionization density (the electron density available at the beginning of each voltage pulse) is lower. With UV illumination, τ is nearly constant (within experimental uncertainty) below 100 Hz.

effect by Pejovic *et al* [12][4]. In extreme cases, the memory effect has been observed over interpulse periods of hours.

Breakdown times are shown in figure 2(*b*) for 30 Torr of argon with and without UV illumination as a function of the PRF for 1500 V pulses. As in the previous result, τ decreases with increasing PRF and illumination reduces τ (relative to the non-illumination value) over the entire range of PRF investigated. τ is larger without illumination due to the lack of (additional) preionization by the UV light. At sufficiently high repetition rates (hundreds of hertz), the mean breakdown times with and without illumination are nominally the same. This result implies that the availability of seed electrons is dominated by the electrons surviving the afterglow following the previous pulse. As repetition rates are decreased below 100 Hz without illumination, the increase in τ reflects the reduction in seed electrons that are available at the onset of each voltage pulse, which, in turn, results in the scatter of the data increasing to unacceptable levels. In the absence of illumination, breakdown could at best be only sporadically

---

[4] For a recent review of breakdown process in low pressure gases, see [12].

achieved at tens of hertz for these experimental conditions (V_0 = 1500 V, 30 Torr argon). With illumination, the mean breakdown time also increases with decreasing repetition frequency but reaches a constant value with small scatter below 100 Hz. In this regime, the availability of seed electrons is dominated by the UV illumination, and changes in τ are due to the formative time lag. The nearly constant value of τ at low repetition frequencies is interpreted as the preionization density provided by the UV illumination being sufficiently small for it not to significantly affect the formative time lag, and yet be adequate to maintain the statistical time lag at a small value.

In light of these results, all the experiments discussed below were conducted with UV illumination and a PRF of 1 Hz. Under these conditions, the statistical error in determining τ is minimized but the PRF is well below the regime in which the measurement of the formative time lag is prejudiced by electrons produced by an earlier discharge pulse.

4. Breakdown in Ar/Xe mixtures

The gas mixture investigated, Ar/Xe, was selected as being representative of a non-chemically reacting mixture having disparate ionization potentials and having many of the qualitative features of Ar/Hg mixtures found in actual lamps. Hg and Xe both have significantly lower ionization potentials and significantly larger momentum transfer (both elastic and inelastic) cross sections than Ar. As such, momentum transfer is dominated by collisions with Ar for low mole fractions of Xe or Hg, while inelastic losses are dominated by collisions with Hg or Xe. This also results in the majority of ions transitioning from Ar to Xe or Hg as E/N decreases as the plasma is established.

The major differences during breakdown between Ar/Hg and Ar/Xe mixtures are likely the contributions from Penning processes. The ionization potential of Ar is 15.76 eV and that of Xe is 12.13 eV, while the energy of the lowest Ar metastable, Ar(4s [3/2]$_2$), is 11.54 eV. As a consequence, this is not a classical Penning mixture in which the lowest lying metastable can ionize the lower ionization potential gas. In Ar/Hg, with an Hg ionization potential of 10.4 eV, all excited states of Ar can Penning ionize Hg. In Ar/Xe mixtures, however, Penning ionization can occur from collisions of Xe with higher excited states of Ar (such as the 4p manifold beginning at 12.90 eV), which are also generally heavily populated throughout the avalanche. Although after breakdown the thermodynamics of Hg may dictate behaviour different from Xe, during breakdown when gas temperatures are low, Ar/Xe is likely a good surrogate for Ar/Hg.

Typical I–V characteristics for pure argon and an Ar/Xe = 90/10 mixture for a 2000 V applied waveform at pressures as high as 90 Torr are shown in figure 3. There are at least three stages of the breakdown process. The first is reaching the threshold value of voltage, or critical E/N, necessary to initiate breakdown. The second is the avalanche process, which creates a conducting channel between the anode and cathode. The final step is the subsequent rise in the plasma channel conductivity and current (yielding a commensurate voltage drop across the ballast resistor), resulting in an observable decrease in the discharge voltage. The formative
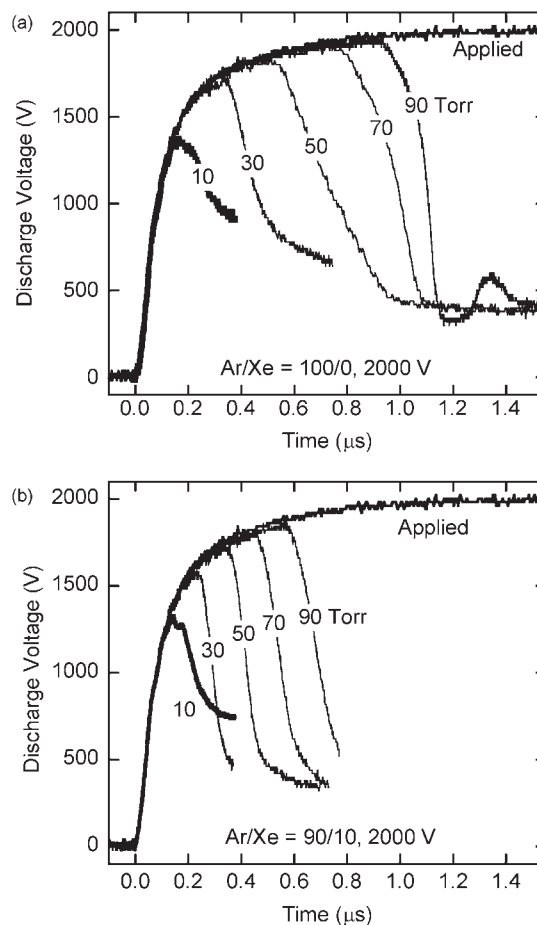
Figure 3. Voltage across the gap for (a) pure argon and (b) Ar/Xe = 90/10 discharges as a function of time for different pressures and V_0 = 2000 V. The formative lag time decreases with pressure in argon but is nearly constant in the Ar/Xe mixture.

time lag constitutes the majority of the time expended during stages 2 and 3. For a given value of E/N, the time expended in the third stage generally scales inversely with pressure since the absolute collision frequencies and electric fields are higher. For the results obtained in pure Ar (figure 3(a)), the decline in the formative time lag that accompanies increasing pressure is shown by the steepening slope of the falling portion of the voltage waveform as the pressure rises from 10 to 90 Torr.

The increase in τ with increasing pressure in argon (figure 3(a)) results from two factors. As there is a critical E/N, $(E/N)_0$, required to initiate the avalanche, a larger voltage is required to obtain breakdown with increasing pressure, and this voltage occurs later in the voltage waveform. The second factor is that, given the voltage waveform in figures 1(b) and 3, the formative time lag may exceed the pulse rise time. This is particularly relevant for the lower gas pressures, and in this situation, E/N will overshoot the critical value $(E/N)_0$. If the formative time lag is short compared with all other timescales, then the value of E/N at which breakdown occurs should be the same at all pressures and equal to $(E/N)_0$. At 10 Torr, the apparent $(E/N)_0$ (based on the maximum voltage prior to breakdown) is 270 Td, whereas at 90 Torr the apparent $(E/N)_0$ is 42 Td. Diffusion losses could play a role in the higher apparent $(E/N)_0$ at lower pressures. For example,

at an E/N, pressure, and discharge tube diameter of 270 Td, 10 Torr, and 1 cm, respectively, the electron diffusion loss time is $\approx 0.2\,\mu$s, which is commensurate with the voltage rise time. In contrast, at a pressure and E/N of 90 Torr and 42 Td, the diffusion loss time is $\approx 2\,\mu$s, which exceeds the voltage rise time and so does not adversely affect breakdown. These results are also consistent with previous observations that breakdown voltages generally increase with an increase in the time rate of change of the voltage [12]. One concludes that the more rapidly applied voltage overshoots the static breakdown voltage by virtue of the formative time lag exceeding the voltage ramp-up time.

Measurements of the prebreakdown and breakdown currents, combined with results from modelling of the breakdown process discussed in part II, suggest that the background electron density at the time of applying the voltage is likely no larger than $10^6\,\text{cm}^{-3}$. For pure argon, the electron density at breakdown can be estimated as the value providing sufficient current for the value of E/N at breakdown such that the voltage drop across the ballast resistor is 10% of its peak value. This value of electron density is calculated to be $\approx 10^{11}\,\text{cm}^{-3}$. Therefore, the electron avalanche must provide an amplification of the electron density of $\approx 10^5$. The time required to provide this amplification, Δt, can be approximated by $\exp(v_\text{d}\alpha\Delta t) = 10^5$, where α is the first Townsend coefficient for ionization and v_d is the electron drift velocity.

The values of α and v_d were calculated by solving Boltzmann's equation for the electron energy distribution for the spatially averaged E/N using a two-term spherical harmonic expansion [13]. When making this estimate, Δt often far exceeds τ, even at the peak values of E/N. For example, for Ar at 90 Torr, the apparent value of $(E/N)_0$ is 42 Td, which gives $\alpha = 1.4\,\text{cm}^{-1}$ and $v_\text{d} = 4 \times 10^6\,\text{cm s}^{-1}$. The estimated breakdown time is $\Delta t = 2\,\mu$s, which is approximately a factor of 2–3 greater than τ. The implication is that the rate of ionization must be larger than that given by the spatially averaged E/N, assuming single-step ionization from the ground state. Multi-step ionization from excited states of Ar would provide additional ionization, though modelling suggests this is not a major contributor [10]. The locally large E/N that occurs in a propagating avalanche front, as encountered in high-pressure streamers, could also provide the required ionization and is the more likely source. These issues will be discussed in more detail in part II.

Voltage waveforms for Ar/Xe = 90/10 mixtures and a 2000 V pulse for total pressures of 10–90 Torr are shown in figure 3(*b*). Mean breakdown times are uniformly shorter for all pressures as compared with the pure argon case. In contrast to pure argon, the duration of the third stage of breakdown, as indicated by the voltage decay times, does not significantly change as a function of pressure. The exception is the 10 Torr case, which likely suffers from excessive diffusion losses.

Mean breakdown times measured as a function of the applied peak voltage for different pressures and Ar/Xe mixtures are shown in figures 4 and 5. Increasing the pulse voltage uniformly decreases τ (and decreases the scatter in the data) for all gas mixtures and pressures. The decrease in τ with increasing voltage is most apparent at the lower values of E/N, where the increase in the ionization coefficient with increasing E/N is most rapid. These trends reflect the voltage waveform reaching $(E/N)_0$ more rapidly with the larger applied voltage.
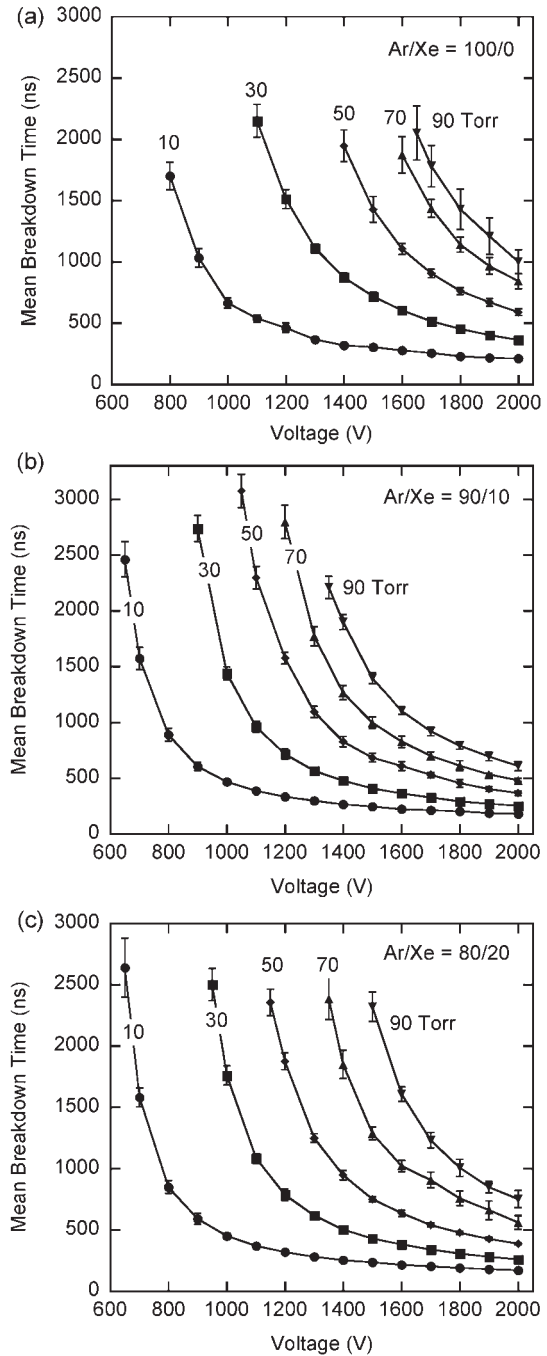
Figure 4. Mean breakdown time as a function of pulse voltage for (*a*) pure argon, (*b*) Ar/Xe = 90/10 mixtures, and (*c*) Ar/Xe = 80/20 mixtures at total pressures between 10 and 90 Torr. Breakdown times decrease with increasing voltage and decreasing pressure.

When replotting the mean breakdown times as a function of the xenon fraction in Ar, as in figures 6 and 7, more definitive trends are apparent. The addition of Xe to Ar initially results in a decrease in τ, and a minimum in the mean breakdown time occurs at Xe mole fractions of 5–15%. This behaviour is likely the result of competition between several processes as the Xe partial pressure is increased. As Xe is introduced, the ionization rate increases quickly, even for small Xe mole fractions, due to its lower ionization potential. Continuing to
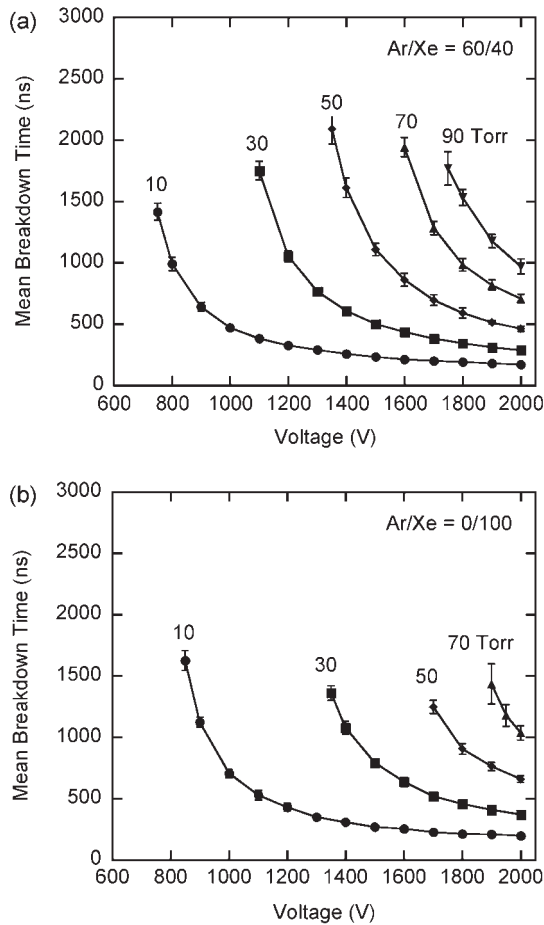
Figure 5. Mean breakdown time as a function of pulse voltage for different pressures and gas mixtures: (*a*) Ar/Xe = 60/40 and (*b*) pure xenon. Large xenon fractions produce longer breakdown times.

add Xe, however, increases momentum transfer and inelastic losses owing to the fact that the momentum transfer cross section for Xe is larger than that for Ar at all electron energies of interest [14, 15]. The first inelastic excitation threshold for Xe is 8.32 eV, whereas the first threshold in Ar lies at 11.6 eV.

Momentum transfer collisions have no threshold energy. Therefore, contributions to the total momentum transfer collision frequency are approximately in proportion to the gas mole fractions. For small additions of, for example, xenon to argon, the influence of Xe on the momentum transfer collision frequency and the electron energy distribution (EED) is correspondingly small. However, the smaller threshold energy for xenon ionization (12.15 eV) compared with that of argon (15.8 eV) enables a significant increase in the rates of ionization at lower values of E/N at which the tail of the EED does not have a significant value at (and above) the Ar ionization threshold energy. As the Xe mole fraction is raised, however, the larger momentum transfer and inelastic cross sections for xenon begin to adversely affect the high energy tail of the EED, and so ionization rates fall in spite of the lower ionization threshold energies of Xe. For moderate additions of Xe, the average electron energy does not appreciably change. It is the dynamics of the tail of the EED that are responsible for the change in ionization rates.
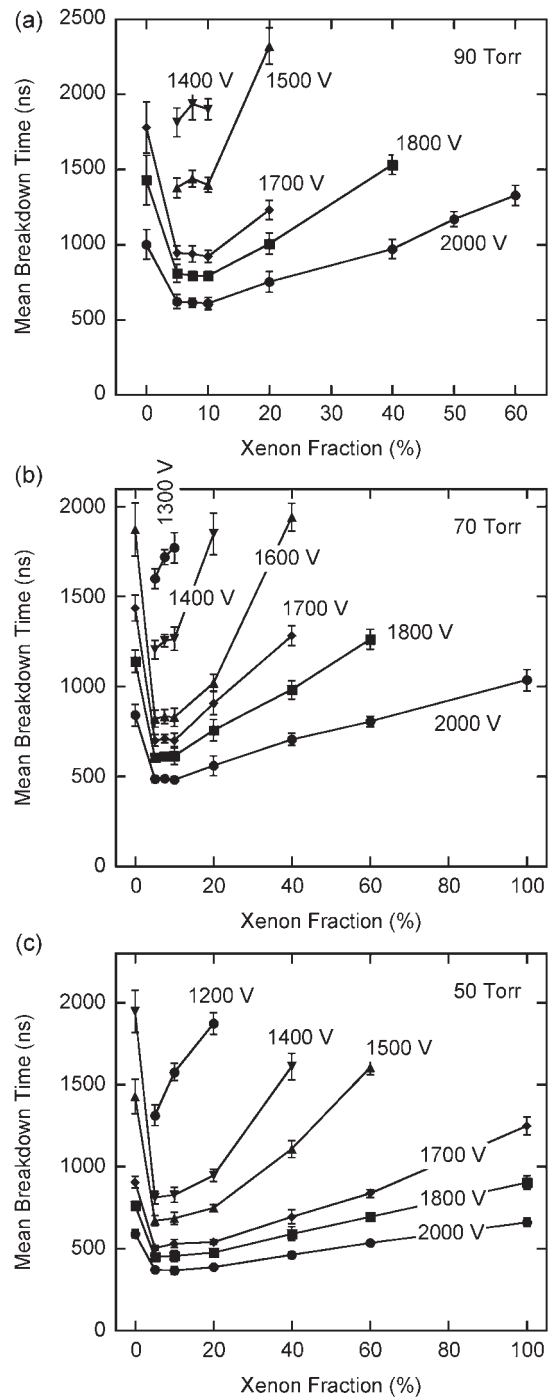
Figure 6. Mean breakdown time as a function of xenon fraction in Ar/Xe mixtures for different values of the pulse voltage: (*a*) 90 Torr, (*b*) 70 Torr, and (*c*) 50 Torr. Breakdown times are shortest with 5–15% xenon addition to argon.

These trends are illustrated in figure 8, in which the electron ionization coefficient (first Townsend coefficient at 1 atm) is shown as a function of the Xe fraction in Ar/Xe mixtures for four values of E/N. Calculated EEDs are also shown at low (40 Td) and high (150 Td) values of E/N for several Xe mole fractions. As noted earlier, these quantities were obtained by solving the steady state Boltzmann's equation for the EED using a two-term spherical approximation [13].
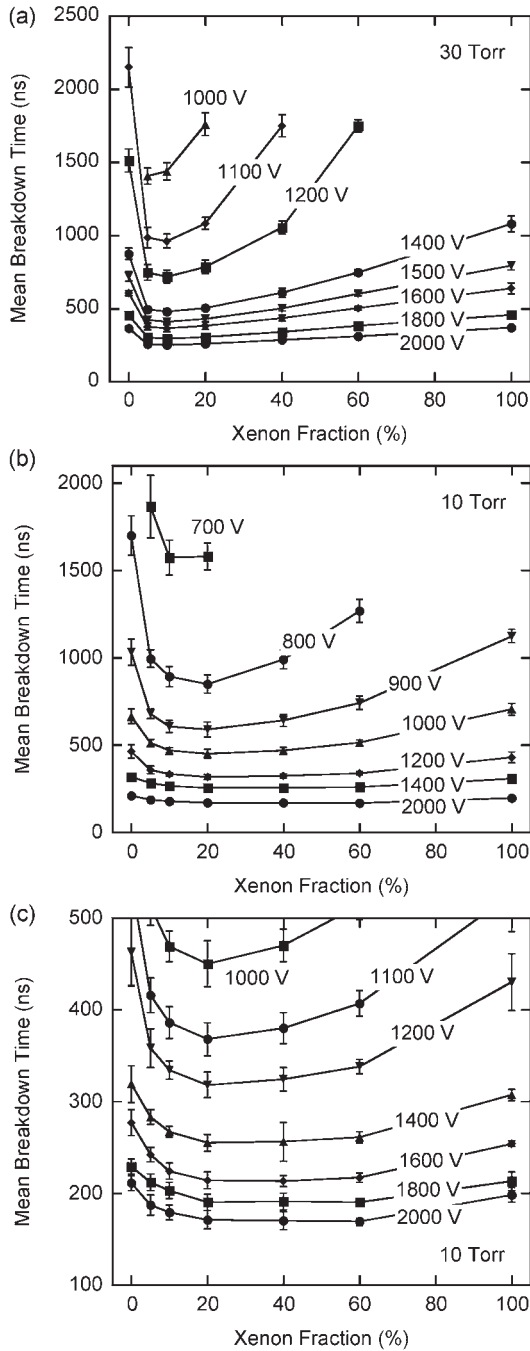
Figure 7. Mean breakdown time as a function of xenon fraction in Ar/Xe mixtures for different values of the pulse voltage: (*a*) 30 Torr, (*b*) 10 Torr, and (*c*) 10 Torr with an expanded view for pulse voltages $\geqslant 1000$ V. Breakdown times are less sensitive to xenon addition at higher values of voltage.

Figure 8. Swarm parameters and EEDs in Ar/Xe mixtures. (*a*) Ionization coefficient at 1 atm as a function of Xe fraction in Ar/Xe for different values of E/N. (*b*) EEDs at 40 Td for different Xe fractions in Ar/Xe mixtures. (*c*) EEDs at 150 Td. The positions of three inelastic collisional thresholds (electron impact excitation of the Xe (6s) states, and ionization of Xe and Ar) are indicated by the dashed vertical lines. At large E/N, the difference in threshold energies for ionization between Xe and Ar is less discriminating, and so the ionization coefficient is a weaker function of the Xe fraction.

At lower values of E/N (figure 8(*a*)), the ionization coefficient increases to a peak at Xe mole fractions of 10–20% and falls rapidly as the Xe partial pressure increases further. The enhancement in the ionization coefficient is large at low E/N since the tail of the EED disproportionately samples the lower threshold ionization cross sections of xenon. For this range of E/N and low Xe mole fractions, the tail of the EED is little affected by the addition of Xe, particularly at lower energies, which determine the electron temperature.

Therefore, increasing the Xe mole fraction produces a net positive (and large) increase in the rate of ionization.

The lower ionization threshold energy of xenon results in a significantly enhanced rate of ionization, but only if the Xe

mole fraction is sufficiently small so as not to significantly increase the rate of momentum transfer or inelastic energy loss. As the Xe mole fraction increases, the tail of the EED is increasingly cut off (truncated) owing to the higher rates of inelastic energy loss and, in particular, electronic excitation. This also results in a drop in average electron energy (or temperature); however, the changes in ionization rates are dominantly a consequence of the dynamics of the tail of the EED. Despite the presence in the Ar/Xe mixtures of a significant Xe mole fraction, damping of the tail of the EED is sufficiently severe so as to reduce the rate of ionization. At large values of E/N, the tail of the EED extends to higher energies and the disparity in the threshold ionization energies between xenon and argon is of less consequence. As a result, at large E/N, the ionization coefficient is a weak function of the Xe mole fraction.

5. Concluding remarks

Breakdown times for electrical discharges in Ar/Xe gas mixtures in an idealized lamp were measured as a function of pressure and gas composition with pulsed excitation of the lamp. UV preionization served to minimize the statistical time lag. Breakdown times for small admixtures of Xe (5–15%) were shorter than those for pure Ar. Larger Xe concentrations yielded values of τ larger than those for pure Ar. These results can be explained by the systematic behaviour of the EED. With the addition of small amounts of Xe to Ar, the tail of the EED is not significantly affected, and so for constant E/N the introduction of lower threshold energy ionization processes in Xe increases the rate of ionization. Large admixtures of Xe, in contrast, truncate the tail of the EED to such a degree that, for a given E/N, the total rate of ionization decreases in spite of the lower ionization threshold. At the higher values of E/N investigated (150 Td), the amount of decrease (or lengthening) in breakdown times accompanying the addition of Xe diminished because the difference between the ionization thresholds of Xe and Ar is insufficient to be distinguished by the tail of the EED.

References

[1] Zaslavsky G, Cohen S and Keeffe W 1990 *J. Illum. Eng. Soc.* **19** 76
[2] Byszewski W W and Budinger A B 1990 *J. Illum. Eng. Soc.* **19** 70
[3] Cohen S, Zaslavsky G and Lester J N 1989 *J. Illum. Eng. Soc.* **18** 3
[4] Gregor P D, Li Y M, Budinger A B and Byszewski W W 1996 *J. Illum. Eng. Soc.* **25** 150
[5] Byszewski W W, Li Y M, Budinger A B and Gregor P D 1996 *Plasma Sources Sci. Technol.* **5** 720
[6] Pitchford L C, Peres I, Liland K B, Boeuf J P and Gielen H 1997 *J. Appl. Phys.* **82** 112
[7] Waymouth J F 1987 *J. Illum. Eng. Soc.* **16** 166
[8] Luijks G M J F and van Vliet J A J M 1998 *Lighting Res. Technol.* **20** 87
[9] Lay B, Moss R S, Rauf S and Kushner M J 2003 *Plasma Sources Sci. Technol.* **12** 8
[10] Bhoj A and Kushner M J 2004 Avalanche process in an idealized lamp. II: modeling of breakdown in Ar/Xe electric discharges *J. Phys. D: Appl. Phys.* **37** 2510
[11] Carleton S, Sienen P A and Stoffels J 1997 *J. Illum. Eng. Soc.* **26** 139
[12] Pejovic M M, Ristic G S and Karamarkovic J P 2002 *J. Phys. D: Appl. Phys.* **35** R91
[13] Rockwood S D 1973 *Phys. Rev.* A **8** 2348
[14] Suzuki M, Taniguchi T and Tagashira H 1990 *J. Phys. D: Appl. Phys.* **23** 842
[15] Suzuki M, Taniguchi T, Yoshimura N and Tagashira H 1992 *J. Phys. D: Appl. Phys.* **25** 50